Korean J. Chem. Eng., 36(1), 166-172 (2019)
DOI: 10.1007/s11814-018-0185-7

pISSN: 0256-1115
eISSN: 1975-7220

pH-triggered intracellular release of doxorubicin from polyaspartamide-encapsulated mesoporous silica nanoparticles

Cheolwon Lim*, Eun-Bum Cho, and Dukjoon Kim*,†**

*School of Chemical Engineering, Sungkyunkwan University, Suwon, Gyeonggi 16419, Korea
**Department of Fine Chemistry, Seoul National University of Science and Technology, Seoul 01811, Korea
(*Received 9 May 2018 • accepted 3 November 2018*)

Abstract−Mesoporous silica nanoparticles (MSNs) conjugating doxorubicin (DOX) via a pH-sensitive cleavable linkage, hydrazine (HYD) were synthesized. MSN-HYD-DOX were encapsulated with the polyaspartamide (PASPAM) grafted with the hydrophilic o-(2-aminoethyl)-o′-methylpoly(ethylene glycol) (PEG) and the cell permeating ligand, biotin (Biotin). The chemical structure of the synthesized MSN-HYD-DOX and PASPAM-g-PEG/Biotin was confirmed using FT-IR and ^{1}H-NMR spectroscopy. The mean diameter of the MSN-HYD-DOX@PASPAM-g-PEG/Biotin nanoparticle was 142 nm and 121 nm, respectively, examined by dynamic light scattering (DLS) and transmission electron microscope (TEM). The HYD bond was effectively cleaved in acidic condition, and thus DOX was released much faster at pH 5.0 than at pH 7.4. The cell viability in MSN-HYD-DOX@PASPAM-g-PEG/Biotin system was much lower than that of the free DOX drug because of efficient intracellular drug delivery associated with the biotin ligand.

Keywords: Mesoporous Silica Nanoparticle, Polysuccinimide, Hydrazone Bond, Doxorubicin

INTRODUCTION

Although human society has become even more developed, the cancer growth rate has not diminished, and the onset age for getting cancer has even reduced. This is because of a variety of factors, including bad food intake habits, smoking, drinking alcohol, toxic environment, and other genetic problems [1]. As the low cure efficiency and the side effect on normal cell are serious problems associated with cancer treatment, there have been many researches to overcome such problems. Targeted drug delivery technique using nanoscaled drug carriers such as micelles [2], liposome [3], dendrimer [4], and inorganic nanoparticles [5] are reported to enhance cancer treatment efficiency, but reduce the side effects via enhanced permeability and retention (EPR) [6,7]. The main problem associated with this technique, however, is the burst release at the initial stage after injection in the blood vessel and the small amount of drug loading inside the carriers, which cannot satisfy the long-term sustained release [8].

Among as-mentioned nanocarriers, MSNs have a unique structure with large pore volume and surface area, and thus the amount of drug can be controlled and maximized to expect a reproducible drug release pattern [9]. The surface of mesoporous silica can be modified to design an optimized drug delivery system compatible with its bio environment [10]. When the surface of MSNs is suitably modified, they can be utilized as pH triggered drug releasing carriers that have potential application in cancer treatment. As the tumor tissue (pH 6.8) and the endosome (pH 5.5) inside cells are in acidic environment, the drug carriers specifically releasing in such acidic environment will bring about the maximized treatment efficiency on cancer cells with the minimized side effect on normal cells [11]. Also, when MSNs are possibly encapsulated with appropriate biocompatible and biodegradable polymers, they may be safely applied as stable and stealthy blood circulating nanocarriers loading many hydrophobic drugs without coagulation when confronted with a variety of protein cells present inside it [12].

Polysuccinimide (PSI) is a typical biocompatible and biodegradable polymer [13]. As it has grafting reactivity by ring opening, a variety of functional groups can be introduced by formation of graft copolymer. When PSI is ring opened, it produces a protein resembling polymer, polyaspartamide (PASTAM) [14,15]. As PASTAM has slower degradation kinetics than a well-known polylactic acid-glycolic acid copolymer (PLGA), more feasible control of biodegradation kinetics is rendered by the control of molecular weight [16].

In this study, drug loaded MSNs were encapsulated with PASTAM not only to inhibit the burst drug release from the bare MSNs, but also to provide stable blood circulation and cell penetration function from the PASTAM. Polyethylene glycol was grafted to PASTAM backbone to provide its surface with hydrophilicity for stable blood circulation [17]. Biotin was also conjugated to PASTAM to provide it with cell penetration function. Doxorubicin (DOX) was loaded in MSNs by chemical conjugation on their surface. As the chemical linkage, HYD between DOX and MSN is cleavable at low pH (acid condition), pH sensitive release pattern is expected [18-20].

MATERIALS AND METHODS

1. Materials

Cetyltrimethylammonium bromide (CTAB, Acros, 99%), tetraethylorthosilicate (TEOS, Acros, 98%), ethyl acetate (Samchun, 99.5%),

†To whom correspondence should be addressed.
E-mail: djkim@skku.edu

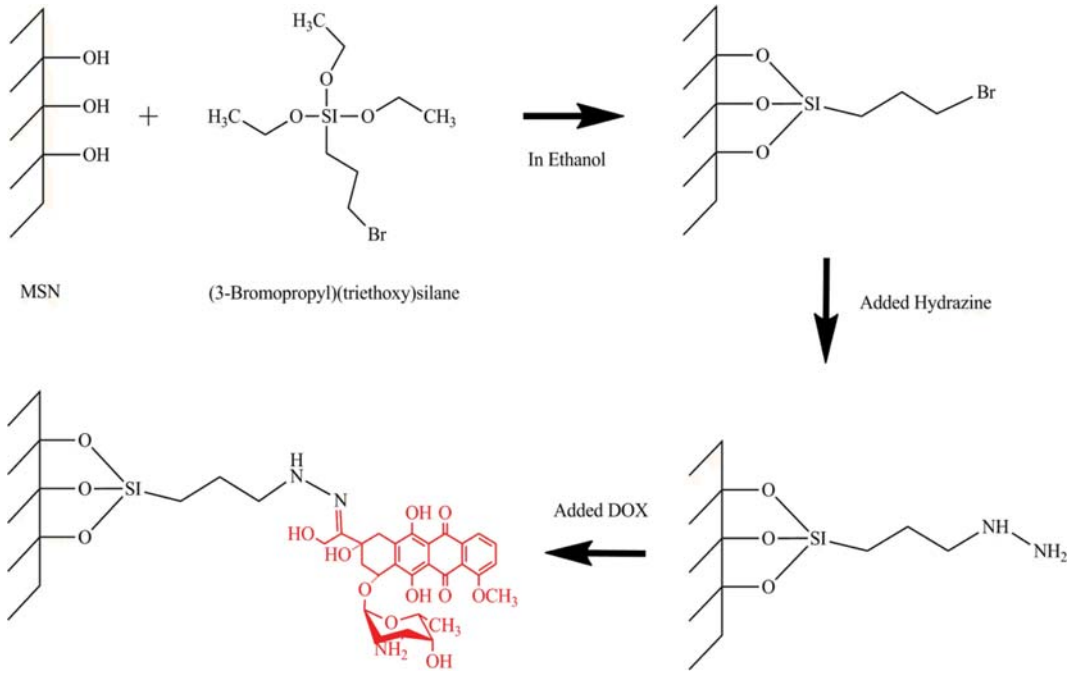

Fig. 1. Synthetic scheme of MSN-HYD-DOX.

3-bromopropyltriethoxysilane (BPS, Gelest, 98%), hydrazine (HYD, 35 wt% in H_2O, Sigma-Aldrich), and doxorubicin hydrochloride (DOX, HPLC, 98%, Sigma-Aldrich) were used for the synthesis of DOX conjugated MSN. O-(2-aminoethyl)polyethylene glycol (PEG, Mw 5000), phosphoric acid (85%, Sigma-Aldrich), L-aspartic acid (Sigma-Aldrich), mesitylene, sulforane (Sigma-Aldrich), N,N-dimethylformamide (DMF, Sigma-Aldrich), anhydrous N,N′-dimethylformamide (DMF, Sigma-Aldrich), ethanol (99%, Samchun, Korea), triethylamine (TEA, Sigma-Aldrich), 4-(dimethylamino)pyridine (DMAP, Sigma-Aldrich), and N,N′-dicyclohexylcarbodiimide (DCC, Sigma-Aldrich) were used for the synthesis of PASTAM. 3-(4,5-Dimethylthiazol-2-yl)-2,5-diphenyltetrazolium bromide (MTT, Sigma Aldrich) was used for the cell binding and viability tests. MCF-7 cells were purchased from Sigma-Aldrich for cell viability test.

2. Synthesis of DOX Conjugated MSNs *via* HYD Linkage (MSN-HYD-DOX)

MSN was synthesized based on the previously reported method [21]. 0.28 g of NaOH and 1 g of CTAB were dissolved in 480 mL water. While the mixture was heated to 80 °C, 5 mL of TEOS was slowly added under stirring. After the mixture was stirred for 2 h, the resulting white precipitate was collected by centrifugation and then washed with plenty of water and ethanol. The pore-generating template, CTAB, was removed by refluxing in HCl and ethanol for 12 h.

The pH sensitive cleavable linker, HYD, was introduced at the surface of MSN. At first, the surface of MSN was functionalized with Br by treatment with BPS. After BPS (300 μL) was added to the MSN colloidal suspension (0.1 mg in 10 mL ethanol), the mixture was refluxed for 3 h. After centrifugation and washing with ethanol, Br-functionalized MSN was redispersed in 10 mL water. HYD was added into the dispersion, and then was stirred for 1 h to retrieve the resulting HYD attached MSN (MSN-HYD) by centrifugation.

DOX was combined with the amine substituted MSNs. After the collected MSN was dispersed in 10 mL methanol, DOX (10 mg) and TEA (0.012 mL) were added. The mixture was shaken for 48 h in a dark environment to induce pH sensitive imine bonding to produce MSN-HYD-DOX. The unreacted DOX was removed by centrifugation, followed by extensive washing with methanol and pH 7.4 buffer solution. During the centrifugation, the supernatant was collected to analyze the loading efficiency of DOX with UV-Vis spectrophotometer at the wave length of 485 nm. The synthetic scheme for the preparation of MSN-HYD-DOX is shown in Fig. 1.

3. Synthesis of PSI and PASTAM Derivatives

PSI was synthesized from L-aspartic acid under acid catalytic condensation reaction. Mesitylene (70 g) and sulforane (30 g) were mixed with L-aspartic acid (25 g) under agitation, followed by the addition of phosphoric acid (15 mmol). PSI was produced from the reaction at 175 °C for 8 h under nitrogen atmosphere. The byproduct of water was removed using a Dean-stark trap. The precipitate in methanol was washed with distilled water until the neutral pH. The final product was dried in a vacuum oven at 70 °C for at least 24 h. The synthetic scheme for the preparation of PSI is shown in Fig. 2.

1 g of PEG and 1 g of PSI were separately dissolved in 10 mL of DMF for each, and the resulting PEG solution was slowly added to PSI. The grafting reaction was performed at 70 °C for 48 h under nitrogen gas. The precipitate product, PEG-g-PSI obtained in diethyl ether was purified using dialysis for 3 d and freeze drying.

Biotin, 2 equiv. of PEG-g-PSI, and 1.1 equiv. of DCC, along with 3 mol% DMAP were mixed in DMF (25 mL). The reaction mixture was kept at 0 °C for 5 min and then at room temperature for 3 h under stirring. After precipitation in diethyl ether, the solvent was removed using a dialysis membrane for 3 d, followed by freeze drying to produce a final PASTAM derivative, PASTAM-g-PEG/

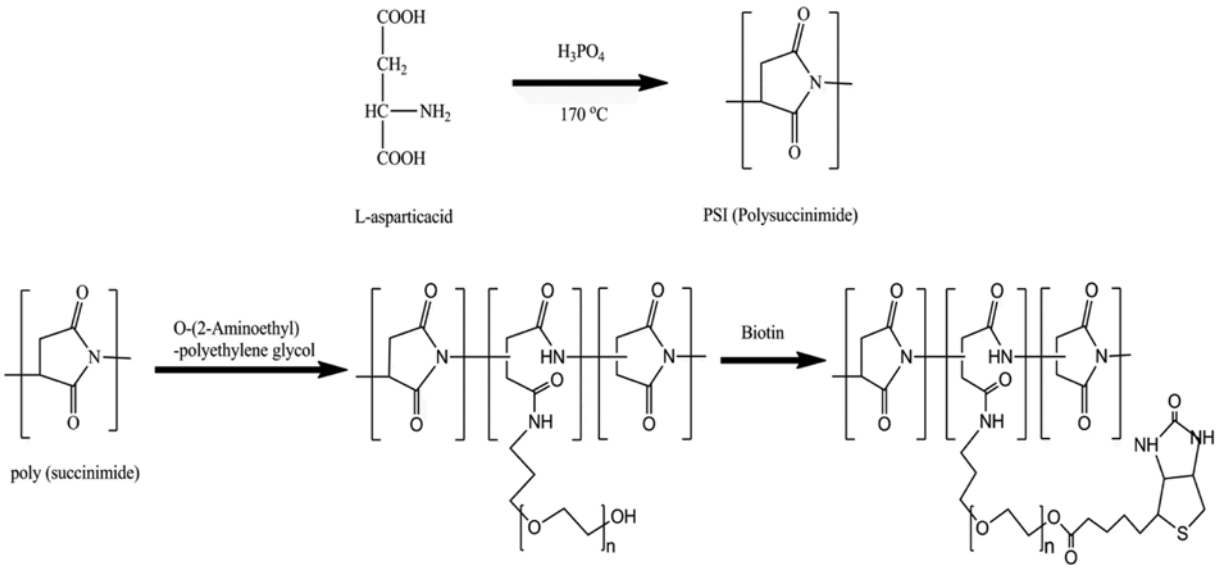

Fig. 2. Synthetic scheme of PASTAM-g-PEG.

Biotin.

4. Synthesis of PASTAM-g-PEG/Biotin Encapsulated MSN-HYD-DOX (MSN-HYD-DOX @PASTAM-g-PEG/Biotin)

MSN-HYD-DOX was dispersed in the PASTAM-g-PEG/Biotin solution and stirred at room temperature for 24 h. The PASTAM-g-PEG/Biotin was bonded with amine groups at the surface of MSN-HYD and the unreacted polymer was removed by dialyzing against water for 3 d. The as-prepared MSN-HYD-DOX@PASTAM-g-PEG/Biotin was collected by centrifugation and then freeze-drying.

5. Chemical and Physical Structure Identification

The chemical structure of PSI and PASTAM-based graft copolymers was confirmed by ^{1}H nuclear magnetic resonance spectroscopy (^{1}H-NMR, Unity Inova 500NB, Varian, USA) and Fourier transform infrared spectroscopy (FT-IR, Bruker IFS-661S, Bruker, USA). The polymer sample was dissolved in DMSO-d_6 or D_2O for ^{1}H-NMR experiment. The dry polymer sample was mixed with KBr powder for FT-IR measurement. The reduced viscosity of the PSI solution was measured using an Ubbelohde viscometer at 25 °C using DMF solvent at 0.5 g dL^{-1}. The molecular weight of PSI was determined from Eq. (1) following the literature procedure [22].

$$n=3.52\ \eta_{red}^{1.56} \quad (1)$$

Transmission electron microscope (TEM, JEM-3010 or JEM-2100F, JEOL, Japan) was used to investigate the size and shape of the MSN-HYD-DOX and MSN-HYD-DOX@PASTAM-g-PEG/Biotin. Samples were prepared in 200 mesh grid by placing the corresponding solution at a desired concentration. The hydrodynamic size and size distribution of the MSN-HYD-DOX and the MSN-HYD-DOX@PASTAM-g-PEG/Biotin particles in solution were investigated by electrophoretic light scattering (ELS, ELS-Z, Otsuka electronics, Japan). A predetermined amount of sample was dispersed in distilled water using an ultrasonifier, and the measurement was performed at 25 °C.

Brunauer-Emmett-Teller (BET) method was used to determine the surface area and size distribution of pores of MSN. Zeta potential was analyzed using electrophoretic light scattering (ELS-Z).

The introduction of each component was confirmed with thermogravimetric analysis (TGA, Seiko Exstar 6000 thermal analyzer. At least 10 mg of sample was heated from 25 °C to 700 °C at 10 °C min^{-1} heating rate.

6. *In Vitro* Release Studies

In vitro release experiments were performed in pH 7.4 and 5.0 PBS buffer solutions. For each release study, 10 mg of DOX-HYD-MSN@PASTAM-g-PEG/Biotin sample was inserted in dialysis membrane with cut-off MW of 12,000 Da. The polymer containing dialysis membrane was placed in PBS solution and maintained at 37 °C, while being stirred at 100 rpm. 1 mL of release (outside) medium was collected for analysis at predesigned time intervals (1, 2, 3, 4, 5, 24, 48, and 72 h). The amount of released DOX was analyzed with a UV-vis absorption spectrophotometer at 485 nm. The drug release studies were performed in triplicate for each sample.

7. *In Vitro* Cell Viability

Cytotoxicity of both DOX conjugated and DOX unconjugated polymer samples were analyzed for MCF-7 cells. The pristine DOX was used as a control system. MCF-7 cells were incubated in a RPMI 1640 medium supplemented with 50 mL of 5% fetal bovine serum (FBS) and 5 mL of 0.5% penicillin/streptomycin under 5% CO_2 at 37 °C. After the cells were cultured in 96-well plates (1×10^4 cells/90 μL per well) for 24 h at 37 °C, 10 μL of the polymer sample prepared was added in each well. After 24 h, 20 μL of MTT solution (5 mg/mL) was introduced and maintained for 2 h at 37 °C in 5% CO_2 incubator. After discarding the culture medium, 200 μL of DMSO was added to dissolve formazan crystal precipitates. After placing in incubator for 30 min, the absorbance was read with a Thermo MK3 ELISA reader at 490 nm, and the statistical mean and standard deviation were used to estimate the cell viability. The relative absorption intensity of the sample was determined based on the absorption intensity of pure PBS solution.

8. *In vitro* Cellular Uptake

The cellular uptake behavior of MSN-HYD-DOX@ PASTAM-

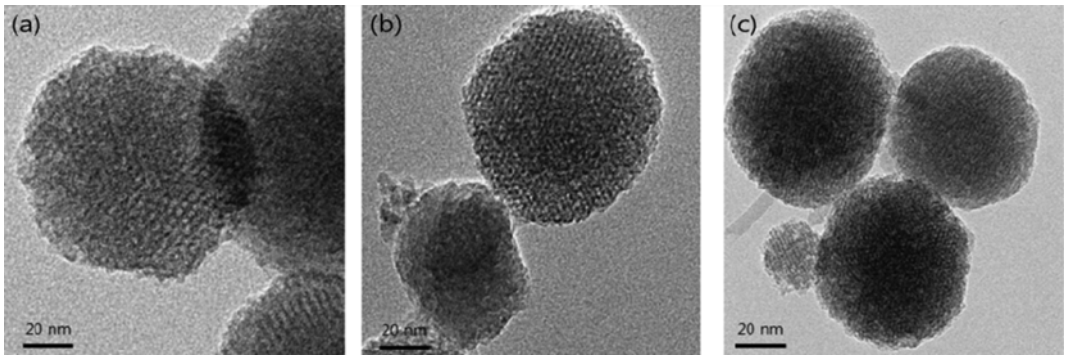

Fig. 3. TEM images of (a) MSN (b) MSN-HYD (c) MSN-HYD-DOX.

g-PEG/Biotin sample was analyzed by fluorescence microscopy. MCF-7 cells were incubated in an RPMI 1640 medium supplemented with 50 mL of 5% fetal bovine serum (FBS) and 5 mL of 0.5% penicillin/streptomycin under 5% CO_2 at 37 °C. After the cells were cultured in 96-well plates (1×10^4 cells/90 μL per well) for 24 h at 37 °C, 10 μL of the polymer sample was added in each well. The cells were fixed using paraformaldehyde and the cell nuclei were stained with 4,6-diamidino-2-phenylindole (DAPI). After washing several times with PBS, the cell nuclei and intracellular delivered DOX were visualized under the excitation wavelengths of 340 nm and 485 nm, respectively.

9. Statistical Analysis

All experiments were performed in triplicate and the resulting data are expressed as the mean value±standard deviations. Statistical analysis was performed using a Student's t-test. $P\leq0.05$ was considered statistically significant.

RESULTS AND DISCUSSION

1. Synthesis of MSN-HYD-DOX

MSNs were synthesized using a positively charged CTAB template under dilute aqueous condition. The TEM image of the synthesized MSN is shown in Fig. 3. The average diameter of MSN was 60±3.2 nm with well-ordered spherical shape, and the average size of MSN was 67±5.1 nm from DLS analysis with the zeta potential of −21.4±2.8 mV.

The subsequent reaction with the excess hydrazine produced MSN-HYD. From ^{1}H-NMR analysis, the protons of the substituted HYD group were well assigned in the NMR spectrum in Fig. 4. Also, the characteristic absorption band from amine group is well illustrated at 1,700 cm^{-1} from FT-IR analysis shown in Fig. 5. From the TEM image in Fig. 3, MSN-HYD has discrete and uniform bulk structure with an average diameter of 70±3.8 nm with well-developed mesopores with an average diameter 5 nm. The average size of MSN-HYD was 78±8.7 nm from DLS analysis with the zeta potential of 16.1±3.2 mV.

The anticancer drug, DOX, was conjugated to the MSN through the pH-sensitive HYD linker to obtain MSN-HYD-DOX. To investigate the conjugation of DOX on MSN-HYD, TGA measurement was employed and the result shown in Fig. 6. Through the temperature increment from 25 °C to 700 °C, 27% and 30% of weight loss was observed in MSN-HYD-DOX and MSN-HYD-DOX@PASTAM-g-PEG/Biotin, respectively, indicating successful loading of doxorubicin and coating of PASTAM-g-PEG/Biotin. From ^{1}H-NMR analysis, the characteristic NMR peaks from DOX were observed

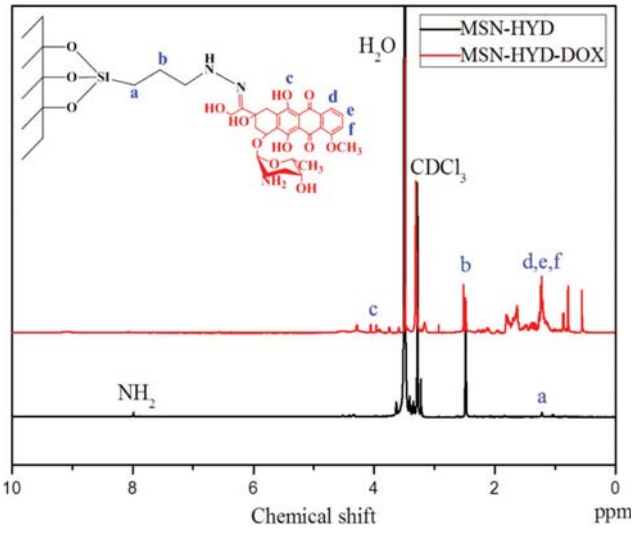

Fig. 4. ^{1}H-NMR spectra of MSN-HYD and MSN-HYD-DOX.

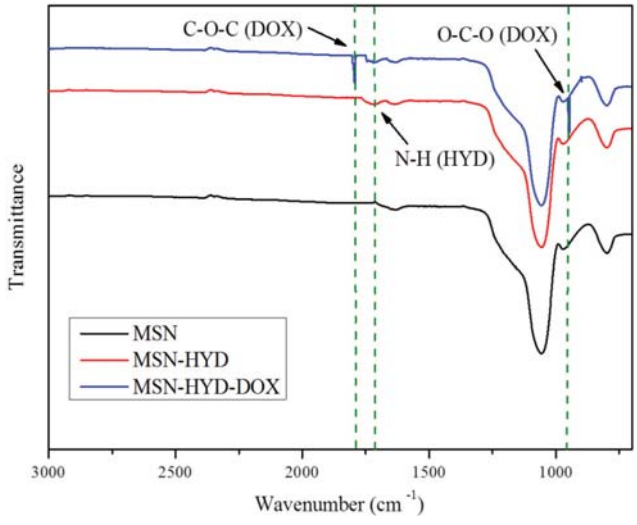

Fig. 5. FT-IR spectra of MSN, MSN-HYD, and MSN-HYD-DOX.

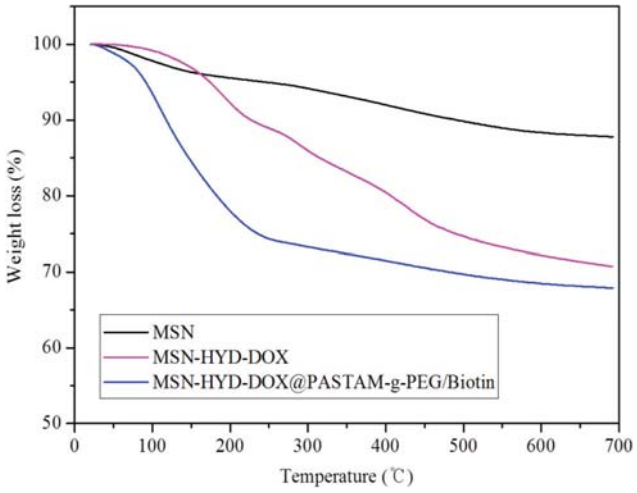

Fig. 6. TGA curves of MSN, MSN-HYD-DOX, and MSN-HYD-DOX@PASTAM-g-PEG.

Table 1. Surface area (S_{BET}) and pore diameter (D_{BJH}) of MSN-HYD and MSN-HYD-DOX

Sample	S_{BET} (m^2 g^{-1})	$D_{BJH\ (nm)}$
MSN-HYD	803.2±32.1	3.7±0.2
MSN-HYD-DOX	201.6±14.4	/

mean±standard deviation; n=3

at 0.7 ppm, 1.1 ppm, 1.5 ppm, and 3.9 ppm. FT-IR spectrum shows the IR absorption band of DOX at 920 cm^{-1}. The average diameter of MSN-HYD-DOX, 102±11.2 nm, was a little larger than that of MSN-HYD from DLS analysis. The particle size measured by TEM was 91±7 nm. The zeta potential of MSN-HYD-DOX was 21.2±2.3 mV, which is higher than that of MSN and MSN-HYD, −21.4±2.8 mV and 16.1±3.2 mV, respectively. The N_2 adsorption-desorption isotherm analysis confirms that the sample has an average pore diameter of 3.7 nm. After the drug DOX was covalently linked onto the nanoparticles, the surface area of the nanoparticles was reduced to 201.6 m^2 g^{-1} from 803.2 m^2 g^{-1}, indicating that a portion of the drug DOX was covalently incorporated inside the mesopores of the nanoparticles. The resulting pore size and surface area from Brunauer-Emmett-Teller (BET) analysis are summarized in Table 1. The mean size of the MSN-HYD-DOX@PASPAM-g-PEG/Biotin was 142±20.1 nm and 121±10.1 nm, respectively, examined by dynamic light scattering (DLS) and transmission electron microscope (TEM).

The loading efficiency (LE) of DOX was defined by the mass of loaded DOX in the unit mass nanocarrier. The amount of loaded DOX was calculated from the UV absorbance intensity of the supernatant, which contained unloaded (free) DOX at 485 nm. The encapsulation efficiency (EE) of DOX was determined from the fractional mass of DOX encapsulated. LE and EE of DOX were calculated from the following equations.

$$LE = \frac{\text{Initial amount of DOX} - \text{Amout of DOX in supernatant}}{\text{Amount of DOX} - \text{loaded nanoparticle}} \times 100 \quad (2)$$

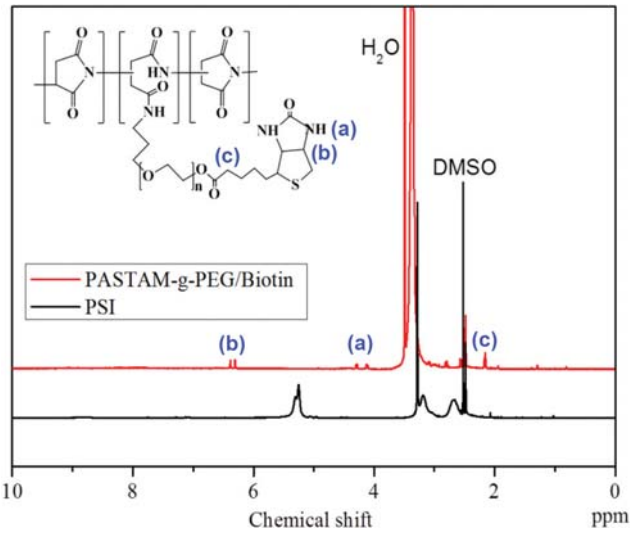

Fig. 7. ^{1}H-NMR spectra of (a) PSI and (b) PASTAM-g-PEG/Biotin.

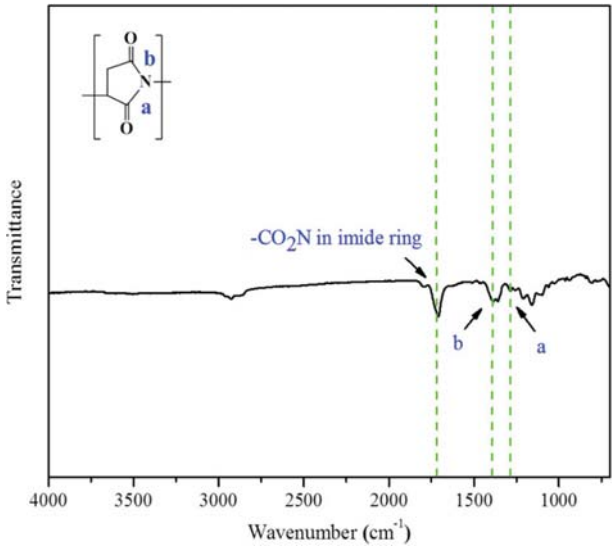

Fig. 8. FT-IR spectrum of PSI.

$$EE = \frac{\text{Initial amount of DOX} - \text{Amout of DOX in supernatant}}{\text{Initial amount of DOX}} \times 100 \quad (3)$$

2. Synthesis of Polysuccinimide (PSI) and PEG/Bio-g-PSI

PSI was synthesized from L-aspartic acid. The reduced viscosity, η_r, was 27 and the corresponding molecular weight is 59,000 g mol^{-1} from Eq. (1). As shown from ^{1}H-NMR spectrum in Fig. 7, the protons in methin group are illustrated at 5.1-5.3 ppm, and the protons in methylene group are at 3.2-3.5 ppm and 2.4-2.5 ppm. The characteristic IR bands of PSI are illustrated at 1,712 cm^{-1}, 1,400 cm^{-1}, 1,215 cm^{-1} and 1,162 cm^{-1} as shown in Fig. 8. Fig. 7 shows the spectra of ^{1}H-NMR of PEG and biotin grafted PSI. The protons present in PEG and biotin are well presented at 2.0-2.2 ppm and 6.4-6.5 ppm in Fig. 7.

3. *In Vitro* Release Studies

The DOX content and drug loading efficiency in the nanoparti-

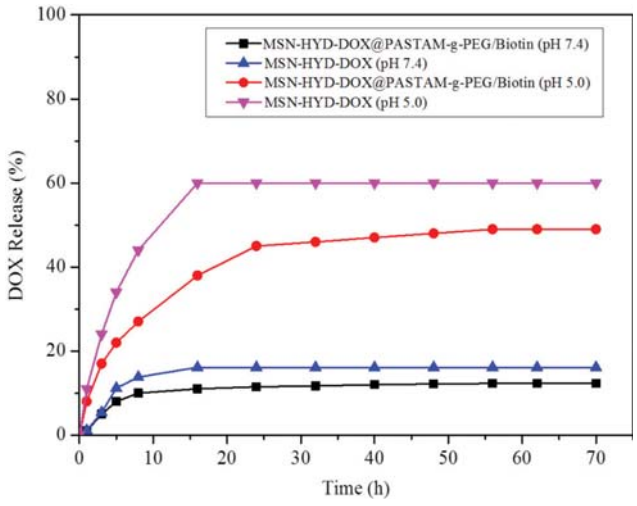

Fig. 9. pH controlled releasing behavior of DOX from MSN-HYD-DOX and MSN-HYD-DOX@PASTAM-g-PEG/Biotin.

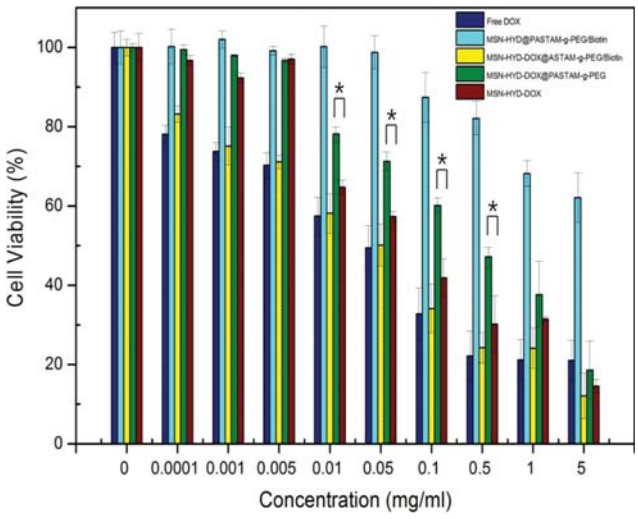

Fig. 10. Cell viability of MCF-7 cells incubated with (a) free DOX, (b) MSN-HYD@PASTAM-g-PEG/Biotin (c) MSN-HYD-DOX, (d) MSN-HYD-DOX@PASTAM-g-PEG and (e) MSN-HYD-DOX@PASTAM-g-PEG-Biotin after 24 h (n=3, *p<0.05).

cle was determined as 20.2±2.5 wt% and 71.8±4.1 wt% from the UV absorbance at 485 nm. The DOX release pattern was analyzed for the self - aggregates formed by MSN-HYD-DOX and MSN-HYD-DOX@PASTAM-g-PEG/Biotin. The pH dependence of DOX release kinetics is shown in Fig. 9. A much faster release behavior was observed under acidic condition (pH 5.0) than under neutral condition (pH 7.4). For MSN-HYD-DOX, 15% of the total DOX loaded was released in about 16 h at pH 7.4 but more than 60% was released in the same period of time at pH 5.0. ForMSN-HYD-DOX@PASTAM-g-PEG/Biotin, system 10% of the total DOX loaded was released in about 30 h at pH 7.4, but more than 45% was released in the same period of time at pH 5.0 because of the diffusional resistance associated with the coated polymer layer. This pH dependence for both systems was caused by the cleavage of the HYD which triggered the release of DOX at acidic condition.

4. *In Vitro* Cell Viability

Various concentrations of MSN-HYD-DOX and MSN-HYD-DOX@ PASTAM-g-PEG/Biotin were co-incubated with MCF-7 to investigate cytotoxicity effect. Up to 5 mg mL^{-1} of nanoparticles was treated to MCF-7, and cell viability was measured with MTT assay after 24 h incubation. The modified results are shown in Fig. 10. When the cells were treated with 0.005 mg of nanoparticles,

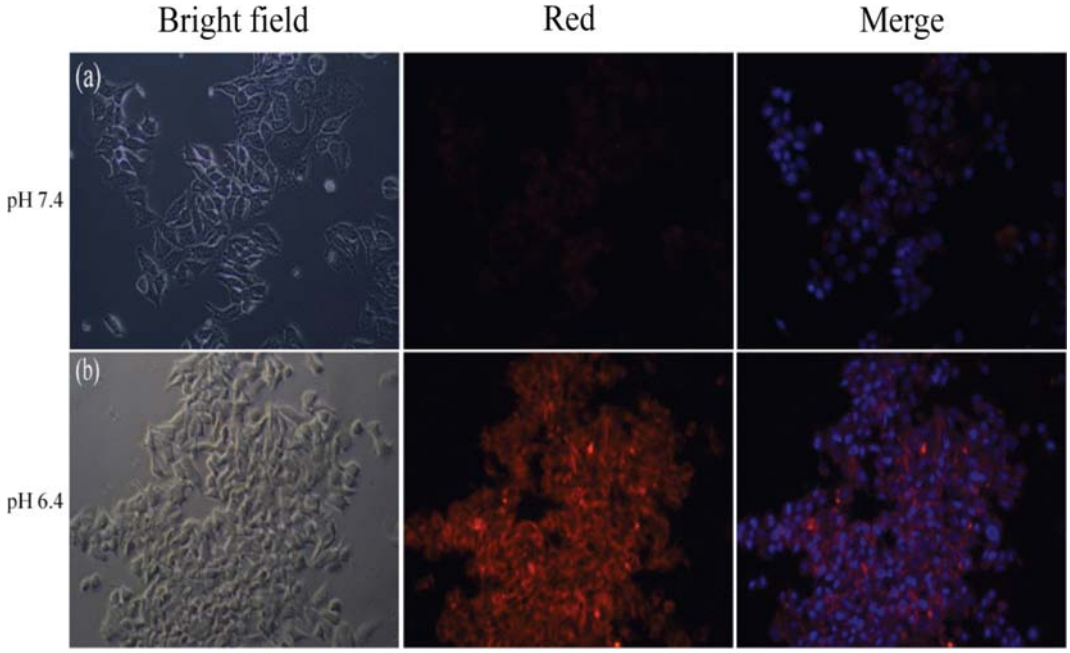

Fig. 11. Fluorescence microscopy images of (a) MSN-HYD-DOX@PASTAM-g-PEG and (b) MSN-HYD-DOX@PASTAM-g-PEG-Biotin after incubation for 3 h at pH 7.4.

MSN-HYD-DOX-treated MCF-7 cells showed the lowest viability compared to MSN-HYD-DOX@PASTAM-g-PEG and MSN-HYD-DOX@PASTAM-g-PEG/Biotin-treated cells. Meanwhile, in case of 0.01 mg of nanoparticle-treated samples, MSN-HYD-DOX@PASTAM-g-PEG/Biotin showed lower viability than MSN-HYD-DOX@PASTAM-g-PEG. This result showed that the Biotin conjugated nanoparticles render more effective drug delivery into MCF-7.

5. *In Vitro* Cellular Uptake

The cellular uptake of synthesized MSN-HYD-DOX@PASTAM-g-PEG/Biotin in the MCF-7 cell was investigated using fluorescence microscopy. After MSN-HYD-DOX@PASTAM-g-PEG/Biotin sample was maintained at pH 7.4 for 3 h, the nuclei of cells revealed blue fluorescence after dyeing with DAPI and the DOX revealed red fluorescence. As shown in Fig. 11, the fluorescence intensity of DOX was higher for the sample with biotin than that without biotin after incubation for 3 h. This result proves that the cellular uptake of MSN-HYD-DOX@PASTAM-g-PEG was improved with biotin.

CONCLUSION

MSN was synthesized and DOX was conjugated to MSNs through HYD to produce MSN-HYD-DOX. Biotin and PEG groups were grafted on the PASTAM backbone as cell penetrating ligand and hydrophilic segments. The average diameter of the PASTAM encapsulated MSN-HYD-DOX, 142±20.1 nm, was slightly larger than that of pristine MSN-HYD-DOX, 102±11.2 nm, from DLS analysis in pH 7.4 aqueous solution. In contrast to the zeta potential of −21.4±2.8 mV of the MSN, that for the MSN-HYD and MSN-HYD-DOX increased to 16.1±3.2 mV and 21.2±2.3 mV, respectively, because of the different surface environment via HYD and DOX. For MSN-HYD-DOX and MSN-HYD-DOX@PASTAM-g-PEG/Biotin systems, DOX was released much faster at pH 5.0 than at pH 7.4 by the cleavage of the HYD under acidic conditions. As MSN-HYD-DOX@PASTAM-g-PEG/Biotin systems exhibited significant cytotoxic effect on MCF-7 cells, the cell viability in this bio-conjugated system was even lower than that of the free DOX drug because of more efficient intracellular drug delivery associated with the biotin ligand.

ACKNOWLEDGEMENTS

This work was supported by the Basic Science Research Program through the National Research Foundation of Korea (NRF) grant funded by the Korean government (MEST) (2010-0027955).

REFERENCES

1. P. Anand, A. B. Kunnumakara, C. Sundaram, K. B. Harikumar, S. T. Tharakan, O. S. Lai, B. Sung and B. B. Aggarwal, *Pharm. Res.*, **25**, 2097 (2008).
2. C. W. Lim, J. H. Park, C. H. Ahn and D. Kim, *J. Mater. Chem. B.*, **3**, 2978 (2015).
3. A. Akbarzadeh, R. Rezaei-Sadabady, S. Davaran, S. W. Joo, N. Zarghami, Y. Hanifehpour, M. Samiei, M. Kouhi and K. Nejati-Koshki, *Nanoscale Res. Lett.*, **8**, 102 (2013).
4. P. Kesharwani, K. Jain and N. K. Jain, *Prog. Polym. Sci.*, **39**, 268 (2014).
5. S. Kango, S. Kalia, A. Celli, J. Njuguna, Y. Habibi and R. Kumar, *Prog. Polym. Sci.*, **38**, 1232 (2013).
6. U. Prabhakar, H. Maeda, R. K. Jain, E. M. Sevick-Muraca, W. Zamboni, O. C. Farokhzad, S. T. Barry, A. Gabizon, P. Grodzinski and D. C. Blakey, *Cancer Res.*, **73**, 2412 (2013).
7. Y. Matsumura, *Drug Delivery System*, **29**, 39 (2014).
8. P. Couvreur, *Adv. Drug Deliver. Rev.*, **65**, 21 (2013).
9. Y. Wang, Q. Zhao, N. Han, L. Bai, J. Li, J. Liu, E. Che, L. Hu, Q. Zhang and T. Jiang, *Nanomedicine: NBM*, **11**, 313 (2015).
10. D. Tarn, C. E. Ashley, M. Xue, E. C. Carnes, J. I. Zink and C. J. Brinker, *Accounts Chem. Res.*, **46**, 792 (2013).
11. S. Yu, G. Wu, X. Gu, J. Wang, Y. Wang, H. Gao and J. Ma, *Colloids Surf., B.*, **103**, 15 (2013).
12. X. Teng, S. Cheng, R. Meng, S. Zheng, L. Yang, Q. Ma, W. Jiang and J. He, *J. Nanosci. Nanotechnol.*, **15**, 3773 (2015).
13. J. R. Moon, M. W. Kim, D. Kim, J. H. Jeong and J. H. Kim, *Colloid. Polym. Sci.*, **289**, 63 (2011).
14. M. Kim, S. W. Shin, C. W. Lim, J. Kim, S. H. Um and D. Kim, *Biomater. Sci.*, **5**, 305 (2017).
15. M. Lee, J. Jeong and D. Kim, *Biomacromolecules*, **16**, 136 (2014).
16. M. Piątkowski, D. Bogdał and K. Raclavský, *Int. J. Polym. Anal. Charact.*, **20**, 714 (2015).
17. E. F. Craparo, G. Cavallaro, M. L. Bondì, D. Mandracchia and G. Giammona, *Biomacromolecules*, **7**, 3083 (2006).
18. Y. Bae, N. Nishiyama, S. Fukushima, H. Koyama, M. Yasuhiro and K. Kataoka, *Bioconjugate Chem.*, **16**, 122 (2005).
19. E. S. Gil and S. M. Hudson, *Prog. Polym. Sci.*, **29**, 1173 (2004).
20. R. Patil, J. Portilla-Arias, H. Ding, B. Konda, A. Rekechenetskiy, S. Inoue, K. L. Black, E. Holler and J. Y. Ljubimova, *Int. J. Mol. Sci.*, **13**, 11681 (2012).
21. X. Li, L. Zhang, X. Dong, J. Liang and J. Shi, *Micropor. Mesopor. Mater.*, **102**, 151 (2007).
22. N. Paolo, A. Guido, B. Franco, C. Francesco and G. Guido, *J. Med. Chem.*, **16**, 893 (1973).